LR-667

The Buckling Behavior of a Central Crack in a Plate under Tension

November 1991

E. Riks / C.C. Rankin / F.A. Brogan

TU Delft

Faculty of Aerospace Engineering

Delft University of Technology

LR-667

The Buckling Behavior of a Central Crack in a Plate under Tension

November 1991

E. Riks / C.C. Rankin / F.A. Brogan

The Buckling Behavior of a Central Crack in a Plate under Tension

by
E. RIKS [1], C.C. RANKIN [2]
and
F.A. BROGAN [2]

1) Faculty of Aerospace Engineering, Technical University of Delft, Delft, The Netherlands
2) Applied Mechanics Laboratory, Lockheed Missiles & Space Company, Palo Alto, California.

ABSTRACT

A finite element procedure is presented for the analysis of the buckling and postbuckling behavior of cracks in plates loaded in tension. The procedure proposed is applied to the problem of the centrally cracked plate in tension where the loading direction is perpendicular to the crack faces. The results of the analysis shows that the buckling deformations can cause a considerable amplification of the stress intensity around the crack tip. This effect, which is due to a redistribution of the stress field in the plate, increases with the length of the crack..

1. INTRODUCTION

A cracked sheet *in tension*, where the crack is aligned perpendicularly to the loading direction, will buckle locally around the crack when the loading exceeds a certain (critical) value. This mechanism is the consequence of compressive transverse stresses that arise in a region along the crack edges. When buckling occurs, the stress field in the plate undergoes a modification, which leads to a change in the behavior of the intensity of the crack tip stress singularity. More precisely, the crack tip singularity is *stronger* in the buckled state than it would have been in the "comparative" unbuckled state at the same value of the load. It is of interest to note that the "buckling" mode of the crack in the plate is similar in form and nature to the "bulging" mode of a longitudinal crack in a thin-walled pressurized cylinder. Both phenomena share the distinction to be governed by a geometrical nonlinear effect (Refs. 1 - 5).

The cracked plate buckling problem has been the subject of study at various occasions in the past but we will refrain from an extensive review. It is here sufficient to mention that the majority of the studies that lay behind us were occupied with the question how to determine the critical state of the plate, i.e., the moment at which buckling takes place, see for instance (Refs. 7 - 17). We will take the point of view here that this problem has been adequately dealt with, at least from the computational point of view, see for example (Refs. 12, 14- 17).

As mentioned, the behavior of the crack after buckling has taken place is governed by a geometrical nonlinear effect. (We will ignore the physically nonlinear effects, i.e., the plasticity effects at the crack tip). This means that the problem must be formulated in terms of a finite displacement plate theory. In the list of references given above, the work of Petyt (Ref. 6) is particularly worthy of mention. He is the only author in this list who took the geometrical nonlinearity just mentioned into account. His work comprises an extensive and interesting study of the behavior of cracked plates, analytically and experimentally. In this pioneering paper, a finite element procedure is described for the analysis of the postbuckling states of the plates with geometrical imperfections[1)]. It furnishes therefore an early example of geometrical nonlinear finite element computations. There is no mention, however, of an attempt to asses how the characteristic crack tip parameter(s) behave along these nonlinear states. Nevertheless, Petyts contribution showed very early on that the finite element approach had a great deal of potential and it is this potential that we want to unfold in the present report.

It must now be clear that the objective of this paper is to go beyond the critical buckling state and to study the postbuckling states of the cracks. To the best of our knowledge, a study of this kind has not been carried out before. The feasibility of a "unified" analysis of this type was demonstrated earlier on two occasions (Refs. 1 & 3), but rather in an ad-hoc way. In these reports, we presented two isolated finite element solutions of a centrally cracked plate loaded into the postbuckling state. The first solution in (Ref. 1) addressed the imperfect plate problem. The second, in (Ref. 3), concerned the same plate but now without imperfections. These particular solutions were derived in a context in which the fracture mechanical aspects of the solutions had to be ignored. They were included in these reports only for the sake of demonstration, for the sake of showing how the present day nonlinear finite element methods codes can be used for the analysis of (nonlinear) cracked plate structures. As such, these exercises can be seen as an preliminary to the present work.

---

1) Shaw and Huang (ref. 17) also addressed the problem of a cracked plate with imperfections. However, the plate theory these authors used is incomplete, rendering their *postbuckling* solutions defective.

The paper is now organized as follows.

-i- Chapter 2 presents an introductory description of the behavior of the centrally cracked plate.

-ii- Chapter 3 describes the methods that are needed for the solution of this problem. Here, special emphasis is placed on the computation of the energy release rates.

-iii- In Chapter 4, the proposed procedure is applied to series of plate configurations.

-iv- Finally, in Chapter 5 we discuss the results of the calculations and present some conclusions that show how the observed behavior of the cracks fits into the notions of classical bifurcation theory.

2. THE CENTRALLY CRACKED PLATE

2.1 General Remarks

For convenience we concentrate on a case that is likely to appear in experiments. A flat plate with rectangular planform: width = 2b, length = 2l and a central crack of length = 2a perpendicular to the axial direction (x), is loaded in tension. The boundary conditions are similar to the conditions which are usually applied in an experiment (see Figure 1). The plate is loaded at the transverse edges but the longitudinal edges are free. We will consider the behavior of this model for a number of geometries determined by the parameters:

$$\mu = \frac{a}{b}; \qquad \kappa = \frac{a}{t}\ ; \qquad \gamma = \frac{b}{l} \tag{2.1}$$

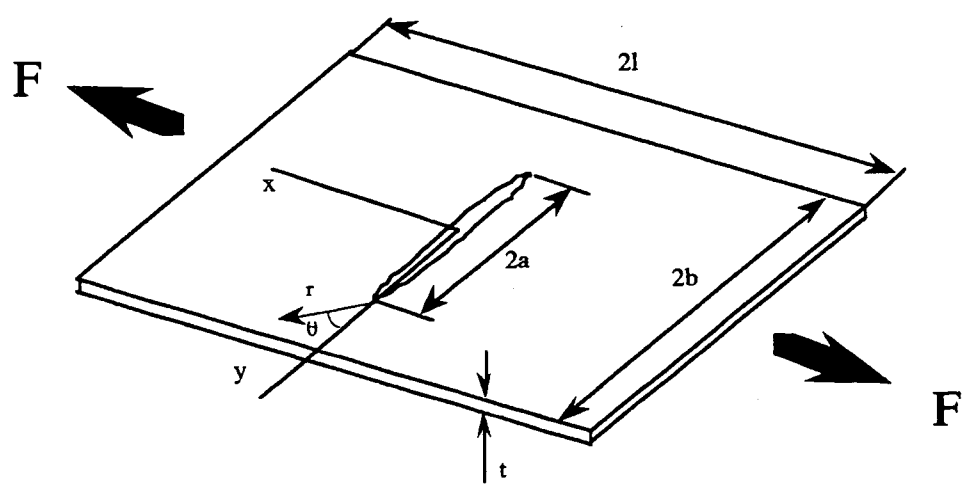

Figure 1 Centrally cracked plate

To illustrate the behavior of this specimen, we consider the out of plane displacement w_c at the center of the crack edge as a function of the load λ [1]. In a qualitative sense, the response of the plate when the load is applied follows a pattern which is rather characteristic for plate buckling problems. At the beginning of the loading process, for $0 < \lambda < \lambda_{cr}$ there is no out of plane displacement. This is the path along the vertical axis denoted by branch I in figure 2. During this phase compressive transverse stresses are building up along a region along the crack edges. Then, at a certain value $\lambda = \lambda_{cr}$, the plate will buckle locally around the crack edges. We can call this process crack-buckling. In the diagram, the development of the buckling deformations is represented by the curve II (figure 2). This is the so called postbuckling path. λ_{cr} Is called the buckling load.

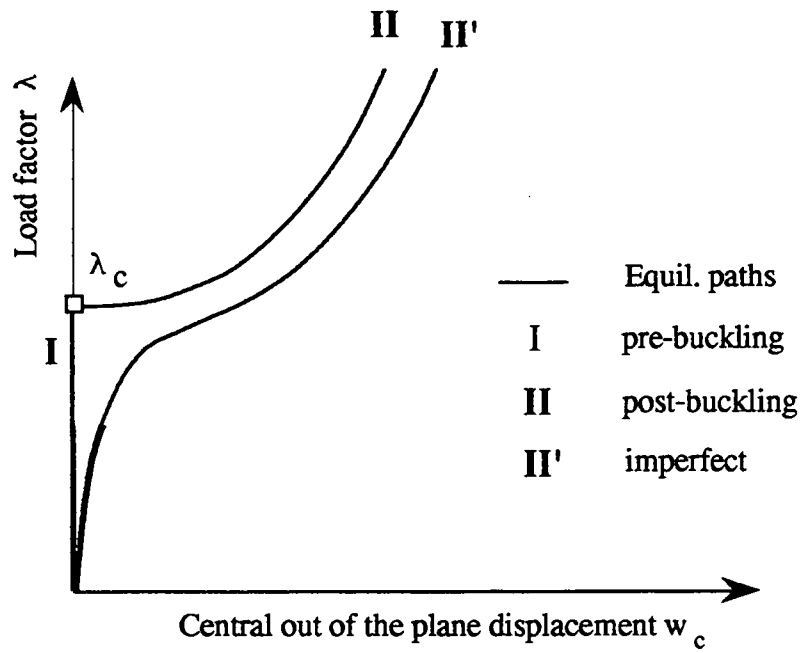

Figure 2 Buckling behavior centrally cracked plate

We note now that the buckling process for this class of problems is stable, because it is still possible to increase the load beyond the critical value λ_{cr}. But as we will show later, at the buckling point, the energy release rate (or the intensity of the crack tip singularity) as a function of the loading undergoes an abrupt change. More precisely, when buckling occurs, the energy release rate will grow faster with the load than it did

[1] It is assumed in these and the following considerations that the crack length 2a does not change during the loading process.

before buckling and the transition point is marked by a jump in the slope of this function, eg.,(Figure 3)[2].

2.2 Perfect versus Imperfect behavior

It is well known that the behavior of the model described above is never observed in experiments. This is due to the fact that there are always deviations from the definition of the problem in the practical situation. For example, in practice the boundary conditions do not precisely match the assumptions on which the model definition is based, or, the plate is not really flat, etc. These deviations or imperfections cause a perturbed behavior of the actual plate with respect to the computational model, and one will observe in the experiment that the actual response of the plate will qualitatively be like the curve labeled by II' in figure 3.

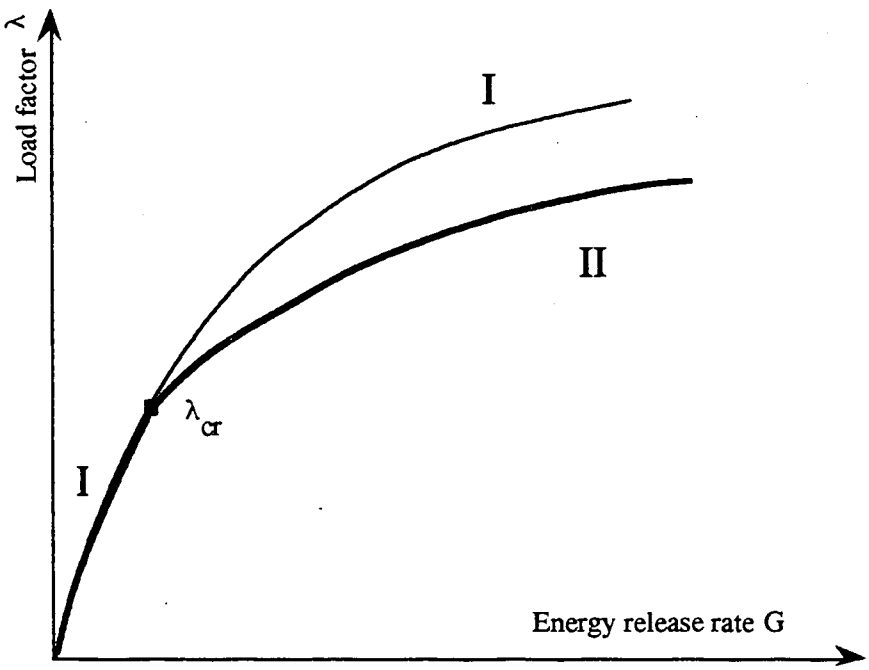

Figure 3 Energy release rate vs. load

The simulation of this natural (or imperfect) behavior with the computational model is relatively easy. It is accomplished by adding imperfections to the geometry of the model (as in (Ref. 1 & 6)). In the remaining part of this paper, however, we prefer to focus *exclusively* on the analysis of the *perfect* plate because it is the principal problem in most of the studies we mentioned earlier.

---

2) In the diagrams and presentation of the results we will follow the convention of elastic stability theory where it is customary to plot the loading vertically.

3. DESCRIPTION OF THE COMPUTATIONAL TOOLS

3.1 Discretization of the Governing Equations

For the analysis of the cracked plate problem we used the STAGS code (= Structural Analysis of General Shells), (Refs.20., 21, 22). This is a code designed for the static and dynamic analysis of shell structures. The equations that are generated by it are a discrete form of thin shell equations that are valid for small strains but finite rotations (Refs.23, 24). This finite element representation is special in that it is formulated on the basis of a co-rotating frame of reference that describes the overall rotation of each individual element (Refs. 21, 22). Within this moving frame of reference, the formulation of the shell equations reduce to a particularly simple form[1)] if the shell has no initial curvature, i.e. when it is a plate. It is a formulation that corresponds to a plate theory which is valid for small strains, and small, (but finite) displacements and rotations (Refs. 21, 22, 24).

Let an arbitrary point of the plate wall in the undeformed state be described by the local Cartesian coordinate system (x, y, z), where x and y measure the distance in axial and transverse direction respectively, and let z be the distance taken along the normal (N) to the plate at (x, y). In addition, let the displacement components that characterize the deformation of the (mid-surface) in these directions be denoted by (u, v, w). It then follows that the Green-Lagrange membrane strain measures are given as:

$$\begin{aligned} \varepsilon_{xx} &= \frac{1}{2}\{\, 2u' + u'^2 + v'^2 + w'^2\} \\ \varepsilon_{yy} &= \frac{1}{2}\{\, 2v^\circ + u^{\circ 2} + v^{\circ 2} + w^{\circ\, 2}\} \\ \varepsilon_{xy} &= \frac{1}{2}\{\, u^\circ + v' + u'u^\circ + v'v^\circ + w'w^\circ\} \end{aligned} \qquad (3.1)$$

The prime denotes here partial differentiation with respect to x, the dot denotes partial differentiation with respect to y; thus $\frac{\partial}{\partial x} = (.)'$; $\frac{\partial}{\partial y} = (.)^\circ$. It is noted that the nonlinear part of the membrane strains are essential for the description of the buckling phenomenon that we are studying here.

The changes of curvature of the plate are given by the linearized, and therefore approximate expressions:

---

1) The use of shell theory implies that we will obtain solutions in the context of plane stress assumptions.

$$\kappa_{xx} = - w''$$
$$\kappa_{yy} = - w^{oo} \qquad (3.2)$$
$$\kappa_{xy} = - w'^{o}$$

which are sufficiently accurate to describe the bending deformations as long as the rotations and the displacement gradients remain small " enough " (Ref. 23, 24).

With these definitions, the description of the state of strain in the plate is completed by means of:

$$\mathfrak{E} = \varepsilon + z\,\kappa \quad \varepsilon = \begin{pmatrix} \varepsilon_{xx} \\ \varepsilon_{yy} \\ \varepsilon_{xy} \end{pmatrix} \qquad \kappa = \begin{pmatrix} \kappa_{xx} \\ \kappa_{yy} \\ \kappa_{xy} \end{pmatrix} \qquad (3.3)$$

The next step is the formulation of the equilibrium equations by applying the principle of virtual work. If $\mathbb{N}$ is the vector of the membrane stress resultants and $\mathbb{M}$ is the vector of the bending stress resultants, this principle can be written in the form:

$$\delta P = 0$$

$$\delta P = \int_S \{\mathbb{N}^t \delta\varepsilon dS\} + \int_S \{\mathbb{M}^t \delta\kappa dS\} - \lambda \int_\Gamma \mathbf{L}_0^t \delta U d\Gamma \qquad (3.4)$$

$$\mathbb{N} = (N_{xx}, N_{yy}, N_{xy})^t \qquad \mathbb{M} = (M_{xx}, M_{yy}, M_{xy})^t$$

where $\delta\mathbf{U}$ = any admissible variation of the displacement field $\mathbf{U} = (u, v, w)^t$. The integrations are extended over the shell surface S and boundary Γ respectively. Note that the last term in (3.4) refers to the external work exerted on the shell by tractions $\mathbf{L} = \lambda\mathbf{L}_0$ along the boundary Γ [2)]. The basic formulation is completed by the through the thickness constitutive equations for a linear elastic shell wall:

$$\mathbb{N} = \mathbf{E}\,\varepsilon \qquad \mathbb{M} = \mathbf{B}\,\kappa \qquad (3.5)$$

where **E** and **B** are the matrices of the generalized membrane and bending stiffnessess of the plate wall.

The STAGS program uses the variational principle Eq.(3.4) as a basis for the discretization process. For details of the plate elements that are available in STAGS we refer to (Ref.20) and the references mentioned there.

---

2) Other types of loadings are not considered here.

3.3 Buckling Equations

After discretization, the equilibrium states of the panel model under load are determined by a set of nonlinear equations that are denoted by:

$$\mathbf{f}(\mathbf{d}; \lambda) = 0 \tag{3.6}$$

where :

$\mathbf{d} \in R_n$ is an n-dimensional vector of nodal displacement variables

$\lambda \in R_1$ is a scalar that represents the load intensity

$\mathbf{f} \in R_n$ is a set of nonlinear functions of $(\mathbf{d}, \lambda)$ that result from the discretization of (3.1 - 3.5)

The solution for the the displacement field of the plate is thus represented by:

$$\mathbf{U} = \mathbf{U}(x, y) = \Omega(x, y)\mathbf{d} \tag{3.7}$$

where Ω is the matrix of shape functions belonging to the finite elements that are introduced.

It is useful to note that the plate problem considered here belongs to a special class of problems where the governing *nonlinear* equations admit one solution set that is *almost linear*. Moreover, this solution can be taken as *linear* for all the applications to be considered here. This means that for a certain, limited range of $\lambda : 0 < \lambda < \lambda_1$ [4] the response of the plate can be written in terms of:

$$\mathbf{d}_I = \lambda \mathbf{D}_0 \tag{3.8a}$$

with $\mathbf{D}_0$:

$$\mathbf{D}_0 = \begin{pmatrix} \mathbf{b}_x \\ \mathbf{b}_y \\ 0 \end{pmatrix} \tag{3.8b}$$

and where $\mathbf{b}_x$, $\mathbf{b}_y$, pertain to the in-plane displacement components. It is noted that this solution is characterized by a *decoupling* between the in-plane displacements and the out of plane solutions so that: $u = \lambda U_0 = \lambda \Xi_0(x, y)$, $v = \lambda V_0 = \lambda \Psi_0(x, y)$ and $w =$

---

[4] We follow here the convention that the plate loaded in tension corresponds to positive values of λ. λ_1 denotes some positive bound.

0. Thus, in this state, to be denoted by **I** in the remaining part of the paper, the plate remains perfectly straight.

Other solutions of the *nonlinear* governing equations (*other* than those represented by **I**) can only have points in common with the linear basic solution (3.8) **I**, if these points are bifurcation points e.g. figure 2. The equations that determine where this occurs along the path (3.8) are the so-called "linearized" buckling equations.

It is a consequence of the linearity of **I**, (3.8), that the displacement field $\mathbf{D}_0$ can be seen as the tangent to the path of solutions **I**. This means that $\mathbf{D}_0$ must satisfy the equations for the tangent to the path ***I*** given by:

$$\frac{d}{d\lambda}\,[\mathbf{f}(\mathbf{d};\,\lambda)] = [D_{\mathbf{x}}\mathbf{f}] \begin{pmatrix} \mathbf{D}_0 \\ 1 \end{pmatrix} = 0 \qquad (3.9^a)$$

or

$$\mathbf{f}_{\mathbf{d}}(\lambda\mathbf{D}_0;\,\lambda)\mathbf{D}_0 + \mathbf{f}_\lambda(\lambda\mathbf{D}_0;\,\lambda) = 0 \qquad (3.9^b)$$

where:

$$[D_{\mathbf{x}}\mathbf{f}] = [\mathbf{f}_{\mathbf{d}};\,\mathbf{f}_\lambda] = [\frac{\partial \mathbf{f}}{\partial \mathbf{d}}\,;\,\frac{\partial \mathbf{f}}{\partial \lambda}\,] = \{\frac{\partial f_i}{\partial d_j}\,;\,\frac{\partial f_i}{\partial \lambda}\}_{\,i,j \in [1,n]} \qquad (3.10)$$

$$[D_{\mathbf{x}}\mathbf{f}] \in R_n \times R_{n+1}$$

denotes the Jacobian of the functions **f**, see Eq. (3.7). Note that the Jacobian $[D_{\mathbf{x}}\mathbf{f}]$ is a combination of the stiffness matrix **K** of the plate evaluated along the basic state **I** :

$$\mathbf{K}(\lambda\mathbf{D}_0;\,\lambda) = \mathbf{f}_{\mathbf{d}}(\lambda\mathbf{D}_0;\,\lambda) \in R_n \times R_n \qquad (3.11^a)$$

and the differential of the loading vector, the vector **l** :

$$\mathbf{l}(\lambda) = \mathbf{f}_\lambda(\lambda\mathbf{D}_0;\,\lambda) \in R_n \qquad (3.11^b)$$

The question of a possible bifurcation from state **I** corresponds thus to the question of the existence of multiple solutions to equation (3.9). To formulate this in formal terms, one assumes the possibility of two solutions $\mathbf{D}_{01}$ and $\mathbf{D}_{02}$:

$$\mathbf{b} = \mathbf{D}_{01} - \mathbf{D}_{02} \qquad (3.12)$$

and derive the equations for the difference **b** :

$$\mathbf{f_d}(\lambda \mathbf{D_0};\, \lambda)\mathbf{b} = \mathbf{0} \tag{3.13}$$

We can show that this set of equations can be approximated by the set of equations:

$$[\mathbf{K}(0) - \lambda \mathbf{K}'(0)]\mathbf{b} = 0 \tag{3.14a}$$

where:

$$\mathbf{K}'(0) = \left[\frac{d\mathbf{K}(\lambda \mathbf{D_0};\, \lambda)}{d\lambda}\right] \tag{3.14b}$$

The matrix **K'** defined by Eq. (3.14b) is the so-called geometric stiffness matrix.

Equations (3.14) are routinely generated by STAGS for any sort of problem that can be modeled by the program. The eigensolutions are found using a subspace iteration method. It computes the eigenvalues λ_i (i = 1, 2, 3, 4,...) in a specified range together with the corresponding eigenmodes (i.e., the buckling modes) b_i. For the problem that is considered here, the lowest positive eigenvalue λ_k of (3.14) (denoted by λ_{cr}) is the critical buckling load.

As it was mentioned in the introduction, in many of the papers cited in the introduction, the derivation and the solution of equations (3.14) is the principal subject. This is particularly true for (Refs. 12 - 17). The differences between these formulations and the STAGS formulation can be found in the details of the discretization technique used and the way the resulting equations are solved.

3.3 Path Following Methods

The equilibrium path **II** (figure 2), which represents the postbuckling states of the plate after the load λ has exceeded λ_{cr}, is a solution of equations (3.7) in which the deformation **d** depends nonlinearly on the factor λ. Usually, such nonlinear equilibrium states can only be computed with specialized methods that obtain points of the equilibrium path **II** step by step using iterative techniques. These methods are called continuation methods, path following methods, or incremental-iterative methods. See for instance (Refs.25 - 28), which also contain further references.

The formulation of the path following methods are usually based on an extended system of equations:

$$\mathbf{f}(\mathbf{d}; \lambda) = 0 \qquad (3.15^a)$$

$$h(\mathbf{d}; \lambda) - \eta = 0 \qquad (3.15^b)$$

that replaces the original system (3.7). The extra equation is introduced to reformulate the problem (3.7) in terms of a new path parameter η by means of which the control of the calculation procedure can be improved. (It furnishes a greater degree of robustness of the iteration process). The scalar function h, by which η is defined, is a function of **d** and λ. In principle, it is reformulated at each new solution step. Note that in this modified formulation, **d** as well as λ belong to the set of unknowns. The solution of the extended set of equations is thus represented by the parametrization:

$$\mathbf{x} = \mathbf{x}(\eta) = \begin{pmatrix} \mathbf{d}(\eta) \\ \\ \lambda(\eta) \end{pmatrix} \in R_{n+1} \qquad (3.16)$$

In this setting, the solutions that the continuation procedure produces can be written as:

$$\mathbf{x}_i = \mathbf{x}(\eta_i)\ ;\ i = 1, 2, 3, ..;\ \eta_1 = 0;\ \eta_2 = \Delta\eta_2\ ;\ \eta_3 = \eta_2 + \Delta\eta_3;\ \text{etc.} \qquad (3.17)$$

where the starting configuration is often the undeformed state:

$$\mathbf{x} = \mathbf{x}(0) = \mathbf{0} \qquad (3.18)$$

The sequence of solution points is obtained by applying a "predictor" - "corrector" process to equations (3.15). At a known solution point $\mathbf{x}(\eta_i)$, the predictor makes an estimate of a new solution $\mathbf{x}(\eta_i + \Delta\eta_{i+1})$ that lays "ahead" for the increment $\Delta\eta_{i+1}$ of the control parameter η. After that, the corrector takes over and finds, by iteration, the new solution to some desired degree of accuracy.

3.4 Bifurcation as a Special Case

The most important part of the calculations that we need for the analysis of the cracked plate, concerns the calculation of the post buckling path **II**. While the computation of the basic state **I** starting from the undeformed state poses no problem, the calculation of the postbuckling path starting from the bifurcation point does. The difficulty concerns the computation of the "predictor", i.e., the initial "guess" that is needed to start the iterations towards the first solution point of the branch **II**.

The first difficulty is that for the construction of this "predictor" the bifurcation point must be located and determined. A second difficulty is that the system matrix **J** is

singular at the bifurcation point, a condition that may lead to divergence of the corrector process if no appropriate measures are taken.

In the cases under consideration, the pre-buckling state is linear and the bifurcation point can directly be determined by solving equations (3.9[a]) & (3.14). We will assume in what follows that this part of the analysis is carried out successfully. Let this solution of the bifurcation point be denoted by :

$$\mathbf{x}_c = \mathbf{x}_I(\eta_c) = \begin{pmatrix} \mathbf{d}_c \\ \lambda_c \end{pmatrix}_I = \begin{pmatrix} \mathbf{d}(\eta_c) \\ \lambda(\eta_c) \end{pmatrix}_I = \begin{pmatrix} \lambda_c \mathbf{D}_0 \\ \lambda_c \end{pmatrix} \tag{3.19}$$

and let the corresponding buckling mode be denoted by $\mathbf{b}_c$. Recall that the buckling mode $\mathbf{b}_c$ stands for the difference between $\mathbf{d}_I$ and $\mathbf{d}_{II}$, the two bifurcating branches when η approaches η_c. With this concept in mind, it is natural to expect that a prediction of a point on the branch **II** can be constructed by setting:

$$\sigma^0_{II} = \mathbf{x}_c + \begin{pmatrix} [\lambda_c + \rho(\Delta\eta_2)]\mathbf{D}_0 + \Delta\eta_2 \mathbf{b}_c \\ \lambda_c + \rho(\Delta\eta_2) \end{pmatrix}_I \tag{3.20}$$

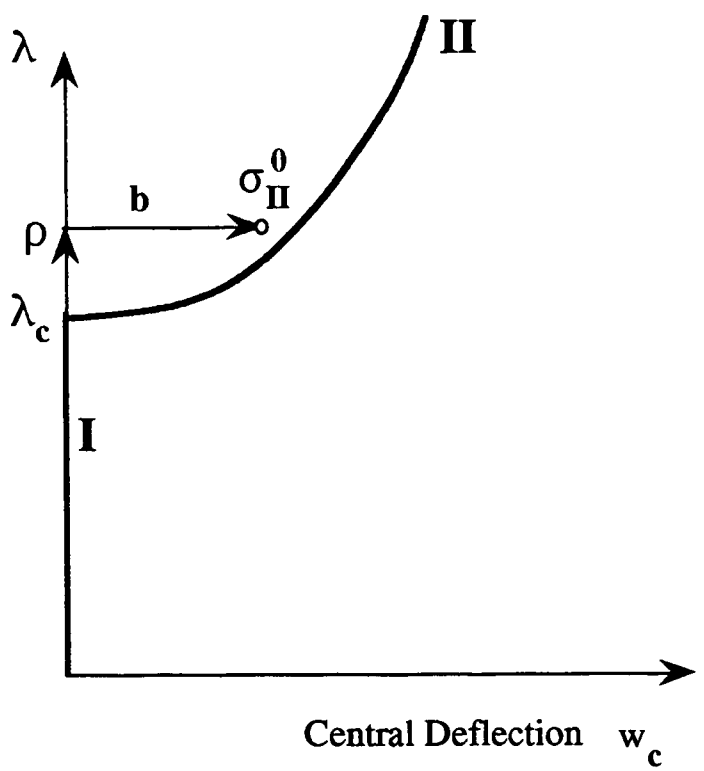

Figure 4 The prediction for the switch to branch **II**

where the path parameter increment $\Delta\eta_2$ into the direction of **II** is prescribed and $\rho(\Delta\eta_2)$ contains information about the growth of the loading in this direction. One can see that a predictor of the type (3.20) is based on a shift from the bifurcation point which consists of a linear combination of the original direction of the path **I** and the direction given by the difference between the two paths **I** & **II** (see also figure 4).

It is of interest to note, that it is at this first step onto **II** that the generalized path parameter η is particularly useful. We will skip the discussion about the manner by which the participation constant $\rho(\Delta\eta_2)$ in (3.20) is computed in general. For this and other details we refer to (Refs. 26, 27, 28).

Let us conclude this description by mentioning that the bifurcation procedure that is implemented in STAGS is not only based on the principle outlined above but also on another, additional feature, which concerns a modification of the corrector equations, i.e., a modification of the equations that perform the iterations towards the new solution on **II**. This modification enhances the robustness of the complete operation considerably. We refer to (Refs.29, 30) for the description of this procedure.

3.5 Computation of the Energy Release Rates

In the continuum description, the total potential energy of the structure is defined by:

$$P[\varepsilon; \lambda; a] = W[\varepsilon; a] - A[U; \lambda; a] \qquad (3.21^a)$$

where

$$\varepsilon = \varepsilon(U)$$

$$W[\varepsilon; a] = \int_S \{\varepsilon^t \mathbf{E}\ \varepsilon dS\} + \int_S \{\kappa^t \mathbf{B}\ \kappa dS\} \qquad (3.21^b)$$

$$A[\mathbf{U}; \lambda; a] = \lambda \int_\Gamma \mathbf{L}_0^t \mathbf{U} d\Gamma \qquad (3.21^c)$$

W is here the internal elastic energy and A = the potential of the external loads. The potential energy is of course dependent on the geometry of the crack, which is the reason why it is included as a parameter in this description.
The energy release rate is defined by:

$$G = -\{\frac{dP}{tda}\}_{\lambda = \text{constant}} \qquad (3.22)$$

where it is tacitly understood that we only deal with straight cracks so that the crack extension is self similar. It is noted that we really need to take the differential of the *total potential energy* i.e., the sum of the internal elastic energy and the potential energy of the externally applied loads. In other words, it is not possible to compute G using the short -cuts that can be introduced in the linear theory (Refs. 31, 32).

In the actual computations presented here, we will use the discrete analog of expression (3.21):

$$P(\mathbf{d}; \lambda ; a) = W(\mathbf{d}; a) - A(\mathbf{d}; \lambda ; a) \qquad (3.23)$$

and determine G from the formal definition:

$$G = -\frac{dP(\mathbf{d}; \lambda; a)}{da} = -\operatorname{Lim}_{\Delta a \to 0} \left\{\frac{P(\mathbf{d}; \lambda; a + \Delta a) - P(\mathbf{d}; \lambda; a)}{\Delta a}\right\} \qquad (3.24)$$

There are several ways to carry out this computation. In the linear range, the available methods are well established (Refs.31, 32). It turns out that they can easily be extended to the nonlinear range. In (Ref.3) we described three examples of these adaptations. A reiteration of the description of two of these methods is given below.

(i) Method 1 (Total Potential Differential by Node Release)

The first method is simply based on the differential form of (3.24):

$$G = -\frac{dP}{tda}\{a = a_1 + \frac{1}{2}\Delta a\} \approx -\frac{P(\mathbf{d}(a_2); \lambda; a_2) - P(\mathbf{d}(a_1); \lambda; a_1)}{t\Delta a} \qquad (3.25)$$

$$\Delta a = a_2 - a_1$$

where a_1 and a_2 are two successive crack lengths along the fracture path that we have to choose close together if we strife for accuracy. The opening process is effected by a node release technique along the crack path. This is an iterative technique because the differential form (3.25) requires the determination of two nonlinear equilibrium states for λ = constant; $a = a_1$ and $a = a_2$ (Refs. 1, 2, 3, 4).

The method described by (3.25) is relatively simple, but it has the drawback that we need to compute at least two successive *nonlinear* equilibrium states. Moreover,

when the structure is large, the numerical values of the two energies that need to be subtracted are large while the difference between the two may be a small, thus leading to a large and possibly unacceptable truncation error. The alternative that we have applied successfully in (Ref.3), and that we will discuss below, is an adaptation to the geometrically nonlinear range of the methods that were proposed by Parks, Hellen and deLorenzi (Refs.33 - 37). It can be seen as the discrete analog of the J - integral method (Refs. 35 - 37).

(ii) Method 2 (Discrete Analog of the J - Integral)

Consider the structure with a crack under its load and assume that the finite element mesh is given. For reasons that will become clear later, the mesh of the structure around the crack tip is divided into three regions (Figure 5). The first, denoted by Ω_1, is enclosed by the contour Γ_1 and contains the crack tip T. The second region is Ω^* an area formed by the strip of elements that border Γ_1 *outside* Ω_1. The third region Ω_2 is the remaining part of the structure. The borderline formed by the element sides connecting the nodes on the boundary between Ω_2 and Ω^* is denoted by Γ_2. The freedoms that are associated with the nodes belonging to Ω^* are denoted by $\mathbf{d}^*$. The freedoms that are connected with the nodes *inside* Ω_1 are denoted by $\mathbf{d}_1$, while those connected with the nodes *inside* Ω_2 are denoted by $\mathbf{d}_2$. With these conventions, the total potential energy of this structure can be written as:

$$P(\mathbf{d};\lambda;\mu) = W_1(\mathbf{d}_1, \mathbf{d}^*; a) + W_2(\mathbf{d}_2, \mathbf{d}^*; a) + W^*(\mathbf{d}^*; a) + \\ - g_1(\mathbf{d}_1, \mathbf{d}^*; \lambda, a) - g_2(\mathbf{d}_2, \mathbf{d}^*; \lambda, a) - g^*(\mathbf{d}^*; \lambda, a) \quad (3.26)$$

where: W_1, W_2, W^*
and
g_1, g_2, g^* = denote the contributions pertaining to the regions Ω_1, Ω_2 and Ω^* of the elastic energy and the potential of the external loads respectively.
λ = the load intensity parameter (which does not play a role in what follows but which is added for the sake of completeness.)
a = the half-length of the crack

The equilibrium equations of the structure are then given by:

$$\frac{\partial W_1}{\partial \mathbf{d}_1} - \frac{\partial g_1}{\partial \mathbf{d}_1} = 0\,;\ \frac{\partial W_2}{\partial \mathbf{d}_2} - \frac{\partial g_2}{\partial \mathbf{d}_2} = 0\,;\ \frac{\partial W_1}{\partial \mathbf{d}^*} + \frac{\partial W_2}{\partial \mathbf{d}^*} + \frac{\partial W^*}{\partial \mathbf{d}^*} - \frac{\partial g_1}{\partial \mathbf{d}^*} - \frac{\partial g_2}{\partial \mathbf{d}^*} - \frac{\partial g^*}{\partial \mathbf{d}^*} = 0 \quad (3.27)$$

It is now assumed that these equations are satisfied for a certain non-zero value of the load, i.e. they are satisfied by the deformation state: $\mathbf{d} = \{(\mathbf{d}_1)^T, (\mathbf{d}_2)^T, (\mathbf{d}^*)^T\}^T$ at $\lambda \neq 0$. At this particular state of deformation, it is of interest to compute the change of the potential energy under a change Δa of the crack length (2a). The change will be invoked by distortion of the existing mesh in accordance with the change of the position of the crack tip T along the projected path of the crack. The particular way this will be carried out is discussed below.

With the prescribed movement of the crack tip, one can decide to distort the mesh in such a way that only the node T changes position, leaving the position of all other nodes unchanged. The distortion of the mesh is in that case restricted to the region of elements that immediately border the crack tip node T. On the other hand, one can also decide to move additional nodal points in the mesh. In principle, the energy release rate is independent of which nodes are moved, provided that the nodes remain on the surface of the model, the boundaries are unaffected, and the crack grows by the prescribed Δa. In practice, however, the results will be affected by discretization errors that stem from a variety of sources. The greatest error can be expected to be found in the rapidly changing stress gradients near the crack tip, with the error diminishing as the distance from the crack tip increases.

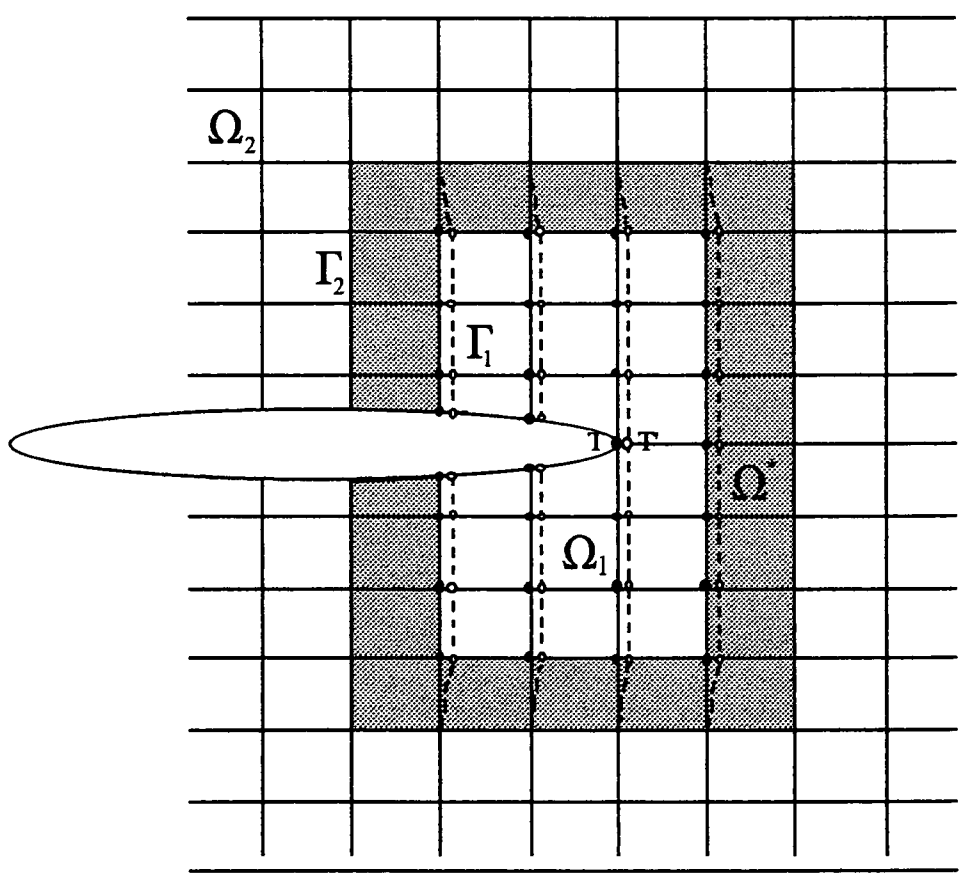

Figure 5 Discrete Analog of the J - Integral

Since we are computing a difference between the energy of the undistorted and distorted mesh, it is advantageous to minimize the number of elements involved, and at the same time, restrict the area that is distorted to be as far from the crack tip as possible. For the flat plate model considered here, we can translate a patch of elements uniformly, including, of course, the crack tip. Then the energy changes are localized to those elements that border the patch. The optimum location of this border is far enough away from the crack tip to avoid severe stress gradients, but not so far as to involve a very large number of elements in the computation.

Specifically, the way the mesh distortion is carried out in STAGS is illustrated in Figure 5. One can see from the figure that the patch of elements Ω_1 is translated *uniformly* to a new position illustrated by the dotted lines in the figure. The crack tip T has moved to T' along the projected fracture path. Distortion of the mesh only occurs in the patch (or string) Ω^* but not in the regions Ω_1 and Ω_2 so that all energy changes are confined to the shaded region Ω^*.

We show this now in formal terms. Straightforward differentiation of the energy expression Eq. (3.26) with respect to (ta) in the direction of the crack axis gives:

$$\frac{dP}{tda} = \left\{\frac{\partial W_1}{\partial \mathbf{d}_1} - \frac{\partial g_1}{\partial \mathbf{d}_1}\right\}\mathbf{d}'_1 + \left\{\frac{\partial W_2}{\partial \mathbf{d}_2} - \frac{\partial g_2}{\partial \mathbf{d}_2}\right\}\mathbf{d}'_2 +$$

$$+ \left\{\frac{\partial W_1}{\partial \mathbf{d}^*} + \frac{\partial W_2}{\partial \mathbf{d}^*} + \frac{\partial W^*}{\partial \mathbf{d}^*} - \frac{\partial g_1}{\partial \mathbf{d}^*} - \frac{\partial g_2}{\partial \mathbf{d}^*} - \frac{\partial g^*}{\partial \mathbf{d}^*}\right\}\mathbf{d}^{*\prime} +$$

$$+ \left\{\frac{\partial W_1}{\partial a} + \frac{\partial W_2}{\partial a} - \frac{\partial g_1}{\partial a} - \frac{\partial g_2}{\partial a}\right\} + \left\{\frac{\partial W^*}{\partial a} - \frac{\partial g^*}{\partial a}\right\} \tag{3.28}$$

where $()' = \frac{d}{tda}$

It follows now from the identities Eq. (3.27) that the first three terms on the right side of above expression vanish. Moreover, the potential energy contributions from the regions Ω_1 and Ω_2 are not influenced by the change of (a) so that the partial derivatives of the functions W_1, W_2, and g_1, g_2 with respect to (a) vanish. Thus there remains:

$$\frac{dP}{tda} = \frac{\partial W^*}{t\partial a} - \frac{\partial g^*}{t\partial a} \tag{3.29}$$

The first term $\frac{\partial W^*}{t\partial a}$ corresponds to the change of internal energy due to the change of stiffness of the region Ω^*. The second term determines the change in the external potential due to the change in the surface integral of this potential. Note that the

resultant forces of the external loading in the domain Ω^* are generally due to a pressure load p, so that this type of loading is not relevant in the case that we are discussing here.
In conclusion it should be mentioned that in the numerical evaluation of the expression (3.29), we make use of the differential form of (3.29) by introducing a finite step Δa, and that we do this backwards and forwards so that the final result is derived from a central difference formula (See also Ref. 3).

4. COMPUTATIONS

4.1 Plate Specifications

The particular dimensions of the plate problem considered here are taken from (Ref.17). They are given by:

Geometrical Data:

Width $2b = 400$ mm ; Length $2l = 800$ mm
Thickness $t = 1.$ mm ; Aspect ratios $\alpha = .2$, thru , .7
$(\alpha = \frac{a}{b})$

Loading : Central load in x- direction

Material constants:

Youngs modulus $E = 70000$ N/mm^{-2}. Poissons Ratio $\nu = .3$

Boundary conditions:

Longitudinal Edges = unrestrained
Loaded Edges = all freedoms restrained, with the exception of the axial displacement u(l, y) which remains uniform with respect to y, but is otherwise free.

4.2 Modeling Aspects

In view of the symmetry of this problem, it is sufficient to consider only one quarter of the plate. In that case, the length and width of the model are *l* and b. Along the two edges $x = 0$ and $y = 0$ symmetry conditions are applied. Along the edge $y = 0$ the symmetry is enforced in a straightforward manner by suppressing v, β_x , β_z (β is the symbol for the edge rotations). At the edge along where the crack can be found (at $x = 0$), the symmetry condition is enforced by means of a set of prescribed displacements along the nodes that are still supposed to be connected with the other

half of the plate. The prescription is there: $u = 0$, $\beta_y = 0$, $\beta_z = 0$. Of course, that part of the edge where the crack is supposed to be is unrestrained.

For this analysis we did not use special elements that are capable of representing the singularity of stress field at the tip. In such cases it is expedient to have a mesh grading that is relatively fine in the neighborhood of the crack. A crude but very convenient way to do this is given by one of the grading options in STAGS which creates structured meshes. Although this is not an elegant way to discretize the model (because it produces many superfluous degrees of freedom), it enables the user to change the model very quickly, and that was for us the most important factor. We considered several meshes in a convergence study and chose a mesh of 40×40 in a format that is pictured in Figure 6.

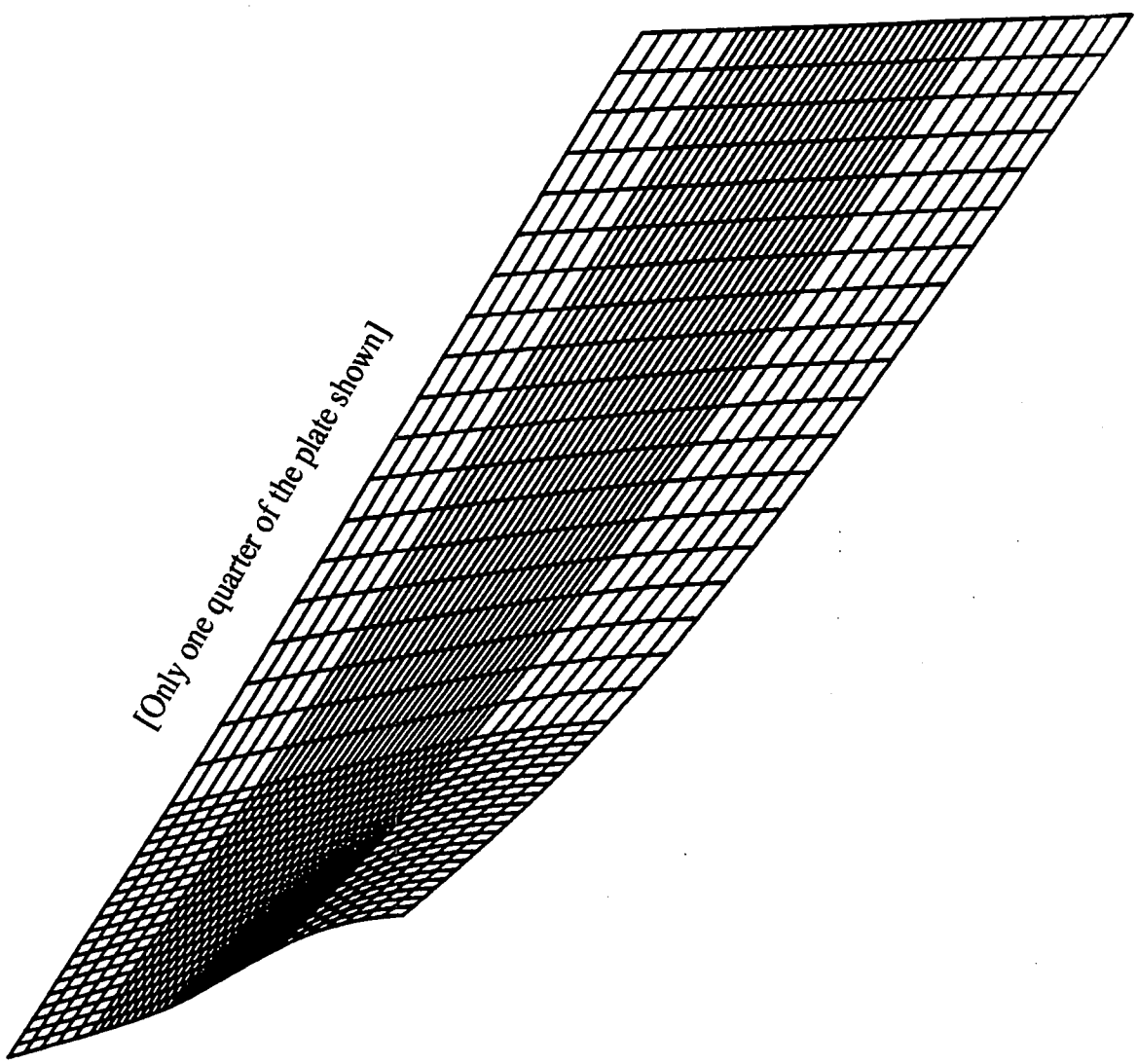

Figure 6 Buckling mode cracked plate

4.3 Buckling Loads

The results of the buckling calculations are presented in Figure 6, 7 and 8. Figure 6 shows the typical shape of the critical mode which is *always* symmetrical with respect to the planes x = 0 and y = 0 (in the cases considered here, see also (Refs. 1, 3, 12-17)). This means that crack behavior that we are studying here belongs exclusively to the class of Mode I type of cracking, *also in the post-buckling states.*

The critical stress $\sigma_{cr} = \frac{F_{total}}{2bt}$ versus the crack aspect ratio $\mu = \frac{a}{b}$ for the range of cracks analyzed here is shown in figure 7. Figure 8 is a repeat of figure 7, but now with the critical stress in non-dimensional form , i.e., $\rho = \sigma_{cr}(\frac{2a}{t})^2 E^{-1}$.

The mesh refinement studies that we conducted seem to indicate that our results for the buckling load accurate up to an order of magnitude of about 3 %. For the larger aspect ratios a/b > .4, excellent agreement is found with the results of computations reported in the literature. For instance, the differences found between the results of (Ref.17) and the present results are at most 6 % where the relative error is defined as:

$$\text{Error} = \left| \frac{\sigma_{present} - \sigma_{ref.}}{\sigma_{present}} \right|.$$

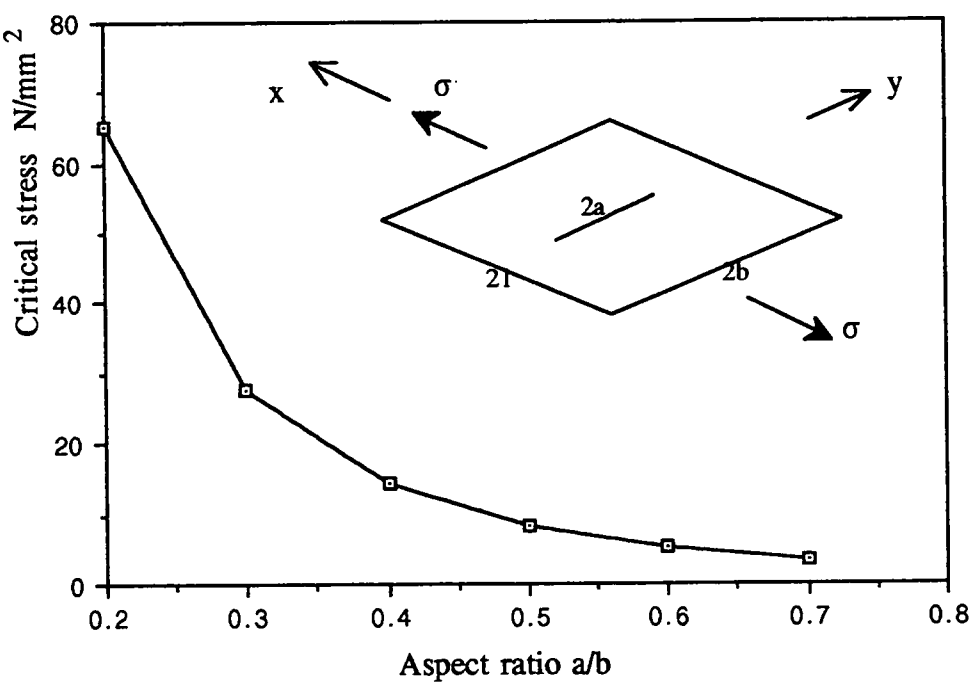

Figure 7 Buckling loads results

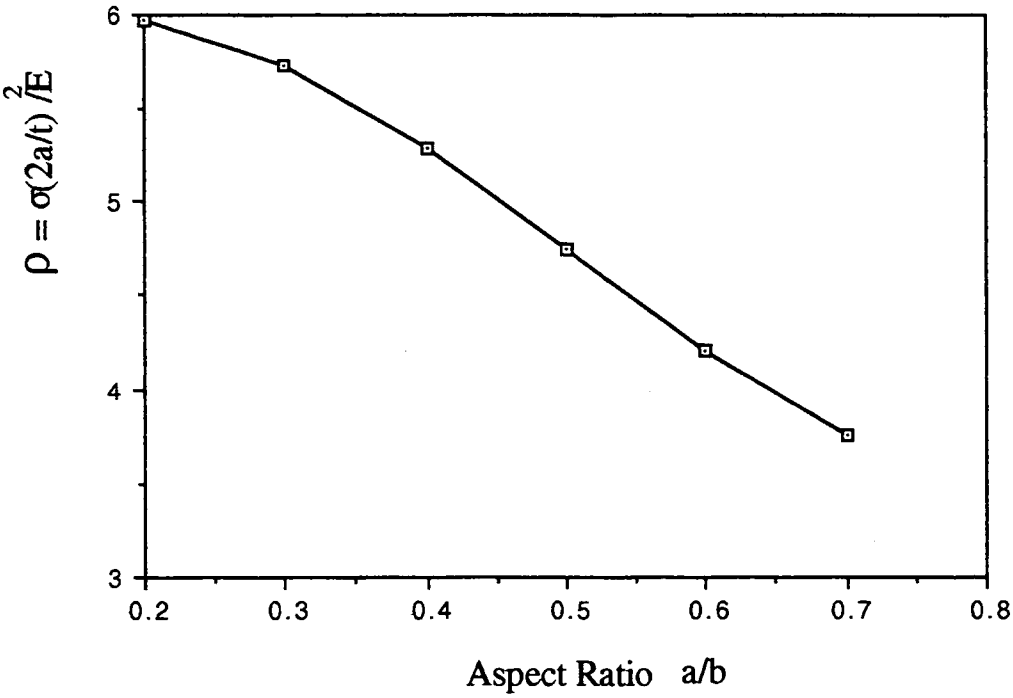

Figure 8. Buckling loads in non-dimensional form

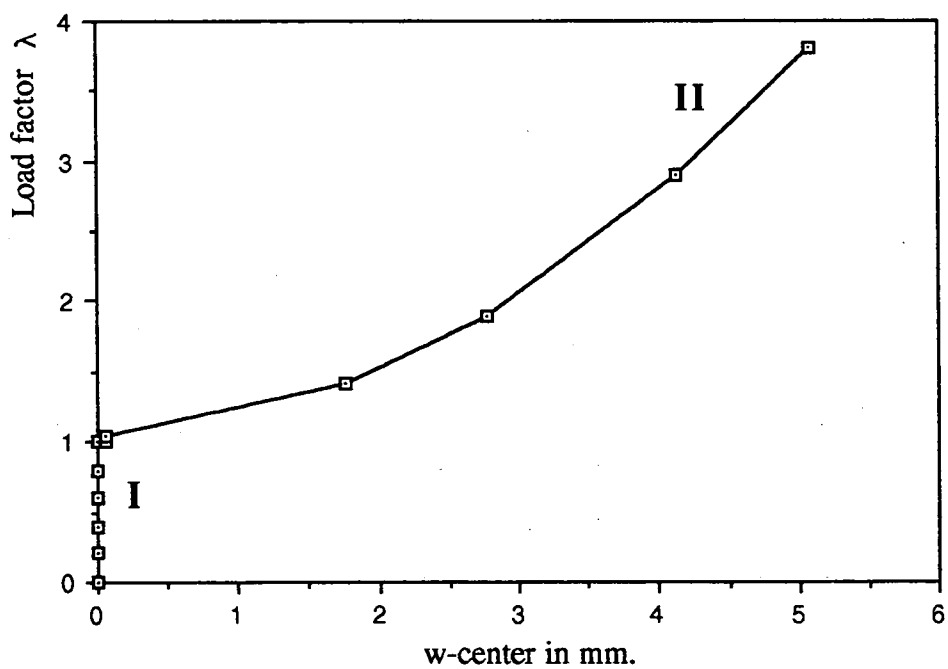

Figure 9 Load vs. center displacement w_c

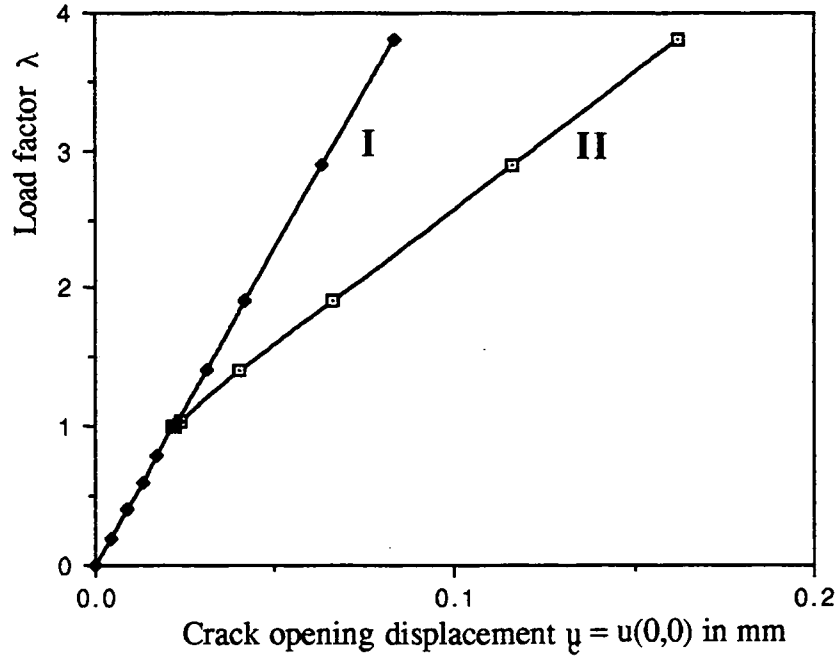

Figure 10 Load vs. center displacement u_c

4.3 Post-Buckling States

Next, we computed the postbuckling behavior of the plate for three choices of aspect ratios $\alpha = a/b$ from the set given in section 3.1, i.e., a/b = 0.2, 0.4, 0.6. In order to save space, we restrict the presentation of the postbuckling calculations to one case (determined by a/b = 0.6) for which the postbuckling solutions are the most pronounced.

Starting from the critical state $\mathbf{D}(\lambda_{cr}) = \lambda_{cr}\mathbf{D}_0$, it was easy to compute the postbuckling equilibrium path following the steps outlined in section 3.3. The calculation of the postbuckling path ***II*** [1] was carried out up to and including the equilibrium point determined by the value of the load of $\lambda_{max} = 4 \times \lambda_{cr}$. The run took 11 steps and no convergence difficulties were encountered. Figure 9 gives the load displacement history for the normal displacement w_c at the center of the crack edge, while in Figure 10 the same diagram is given for the in-plane displacement $u_c = u(0, 0)$ at the edge. Note that in these graphs the load factor λ is defined as: λ = [load]/[critical (buckling) load]. It should be mentioned that the deviation from the straight line of the curve ***II*** that can be seen near the bifurcation point is due to the

[1] From now on we will denote the pre- and postbuckling states by *I* and *II* respectively, in order to avoid confusion with the symbols for mode I and mode II cracking. Note, that this practice is not followed in the figures because there danger of confusion does not exist.

circumstance that the bifurcation point is represented in the figure by the solution of the *approximate* buckling equations (3.14[a]) instead of the exact equations.

As can be judged from figure 10, in the postbuckling state the in plane displacement u_c at the center of the crack is still a linear function of the load factor λ, at least, in good approximation. The same observation applies to the end displacement: $u_E = u(x, y = .5\ell)$ a plot which is not shown here. The load-displacement response of the cracked plate in tension is thus very similar to that of a simply supported plate in compression for the range of load factors considered here (Refs. 18 &19). We defer a further discussion of this behavior to section 5.2.

4.5 The Energy Release Rates

To compute the energy release rates along the path ***II***, we used the contour integral method (2) in section 3. We note here that the calculation of G was first tested in the linear range and compared with the formula for a centrally cracked plate given by Feddersen (Ref.31):

$$G = \frac{K_I^2}{E} \tag{4.1a}$$

$$K_I = \sigma_\infty \sqrt{\pi a} \sqrt{[\sec\{\frac{\pi a}{2b}\}]} \tag{4.1b}$$

with K_I the symbol for the mode I crack intensity factor.

It turned out that the STAGS results for the linear case differed less than 2% from the values determined by this analytical solution. We note that this corresponds to a difference the order of magnitude of the error of the formula itself.

The results for the postbuckling states are plotted in Figure 12. If we boldly use the formula (4.1) to approximate the Mode I stress intensity factor K_I in the buckled state ***II***, the results are transformed to the graph given in figure 13. This form of the postbuckling solutions is revealing because it seems to indicate that the Mode I stress intensity factor K_I along the postbuckling path is still a linear function of the load (to a good approximation), just as it is in the linear pre-buckling state ***I***. Consequently, our results seems to suggest that it is possible to represent the solutions for the centrally cracked plate in the form of :

$$\textit{I}: \quad \lambda \le 1: \ [K^*_I]_{\textit{I}} = f_{\textit{I}}(\lambda)\Theta(a,b) = \lambda \sigma_{\infty cr} \sqrt{\pi a} \sqrt{\sec\{\frac{\pi a}{2b}\}} \tag{4.2}$$

where: $\lambda = \frac{\sigma_\infty}{\sigma_{\infty cr}}$; $\sigma_{\infty cr}$ = average critical stress at the loaded edges (Ref.29).

$$\textit{II}: \quad \lambda > 1: \ [K^*_I]_{\textit{II}} = f_{\textit{II}}(\lambda)\Theta(a,b) = [1 + (\lambda - 1)\kappa^{-1}]\sigma_{\infty cr}\sqrt{\pi a}\sqrt{\sec\{\frac{\pi a}{2b}\}} \quad (4.3)$$

where, in (4.3), κ is a positive constant, smaller than unity, which depends on the specific plate geometry, crack length, boundary and loading conditions at hand. Note that κ can be determined by a curve fit applied to the results in figure (12).

As mentioned, equation (4.3) can only be considered to be an approximation for the stress intensity factor K_I (λ) along the loading path *II*. To what extent this approximation can be trusted will be discussed in the following chapter. It can already be mentioned that for the cases considered here (4.3) is a very good approximation.

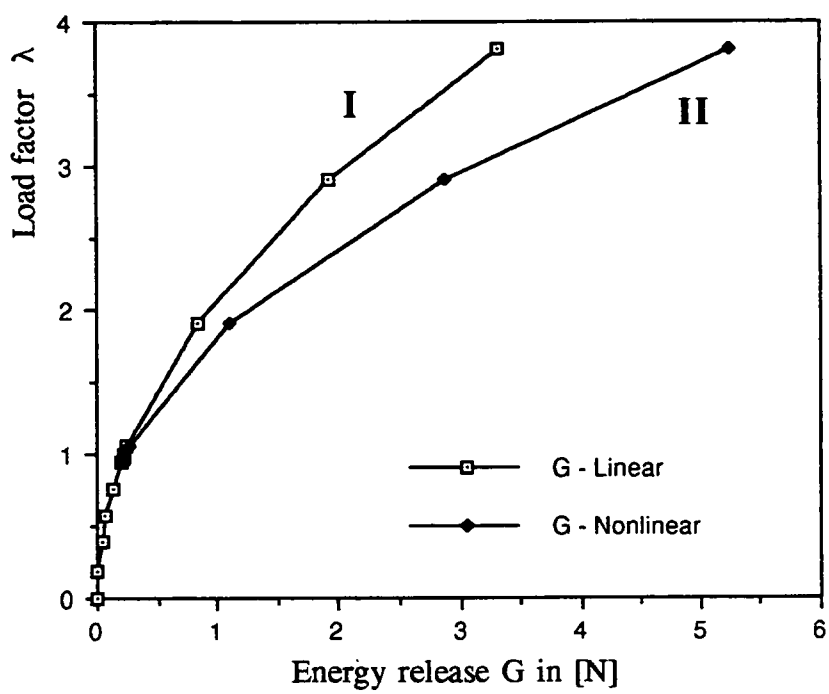

Figure 11 Energy release rate vs. load

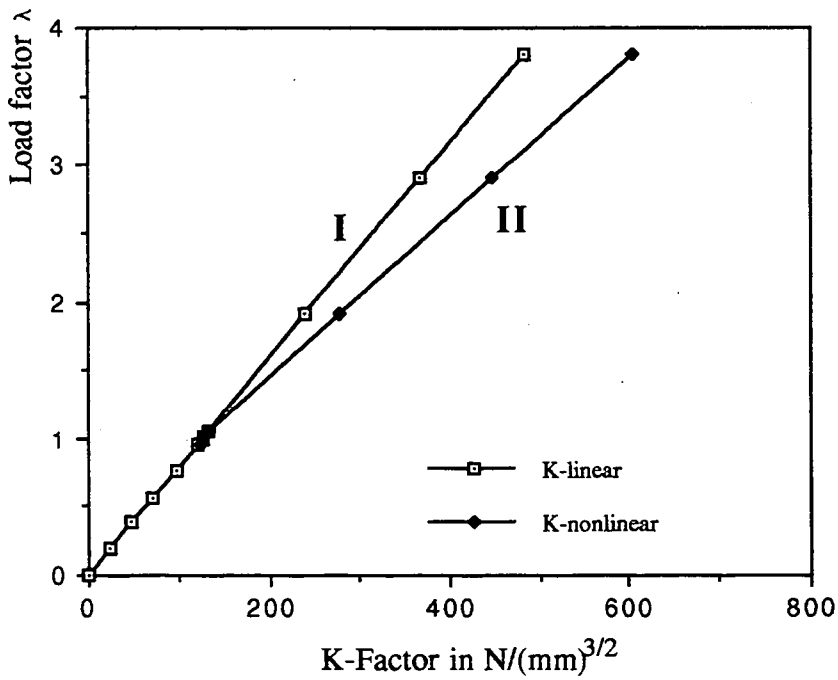

Figure 12 K_I - Factor (defined by $K_I = \sqrt{GE}$) vs. load

5. DISCUSSION AND CONCLUSION

5.1 On the Global Form of the Solutions

The behavior of the energy release rate of the crack at buckling can be brought in a wider perspective (in a qualitative sense) with the help of the general results of the buckling & postbuckling theory for elastic structures (Refs.18, 19). In the following discussion we will introduce these results for as far they are needed to support the development of our arguments.

It is useful to write the total displacements in the postbuckling state as the sum of the pre-buckling displacements $\lambda \mathbf{D}_0$ and the buckling displacements **d**:

$$\mathbf{D}_{total} = \lambda \mathbf{D}_0 + \mathbf{d} \qquad (5.1)$$

The change of the total potential energy ΔP of the plate in going from state **I** to state **II** is then defined as :

$$\Delta P(\mathbf{d}; \lambda) = P(\lambda \mathbf{D}_0 + \mathbf{d}) - P(\lambda \mathbf{D}_0) \qquad (5.2)$$

where P = the function that we introduced at (3.23). The Taylor expansion of this function with respect to λ can formally be written as:

$$\Delta P(\mathbf{d};\lambda) = \Delta P^0{}_2(\mathbf{d}) + \lambda\,\Delta P'_2(\mathbf{d}) + \lambda^2\Delta P''_2(\mathbf{d}) + .. \\ + \Delta P^0{}_3(\mathbf{d}) + \lambda\Delta P'_3(\mathbf{d}).. + \Delta P^0{}_4(\mathbf{d}) + .. \qquad (5.3)$$

where ΔP_i i = 2, 3, 4 denote the quadratic, cubic and quartic parts of the energy in terms of the additional (buckling) displacement **d** and ( )' denotes the derivative with respect to λ: $( )' = \frac{\partial}{\partial\lambda}$. It turns out, by inspection, that for all practical purposes this expansion can be truncated to:

$$\Delta P(\mathbf{d};\lambda) = \Delta P^0{}_2(\mathbf{d}) + \lambda\,\Delta P'_2(\mathbf{d}) + \Delta P^0{}_3(\mathbf{d}) + \Delta P^0{}_4(\mathbf{d}) \qquad (5.4)$$

which is a form of the potential energy which is characteristic for flat plates experiencing small strains, moderate but finite displacements and rotations. It is noted that the quadratic term $\Delta P^0{}_2$ in this expansion is positive definite. On the other hand, the term $\lambda\Delta P'_2$ is indefinite in our case. It represents the coupling between $\lambda\mathbf{D}_0$ and **d** in the expansion and it turns out that is the only term coupled with λ that needs consideration. (The terms belonging to higher order powers of λ are either negligeable or identically zero (Ref.24).)

If $\mathbf{b}_c$ is the buckling mode determined by equations (3.14[a]) it is possible to write the solution for the buckling displacements in terms of a perturbation expansion:

$$\mathbf{d} = \eta\mathbf{b}_c + \eta^2\mathbf{v} + O(\eta^3) \qquad (5.5)$$

(Refs.18, 19)

where **v** is the so called second order perturbation field and η is the parameter that represents the growth of the buckling displacements **d**.

It turns out that the second order displacement field **v** is determined by a linearized problem that can be considered to correspond to the cracked plate (as it is studied here), but now loaded with a *modified* system of loads and boundary conditions. The new load system and boundary conditions are determined by the bucklingmode $\mathbf{b}_c$. We will not describe this additional problem here because it is not strictly necessary for the present argument. It should be kept in mind, however, that **v** is again a membrane mode so that it has only components in terms of the in-plane displacements (u, v). This mode represents a part of the solution (5.5) that takes care of the redistribution

of stresses in the plate once the out of plane displacements (w), contained in ηb_c, start to grow and become finite.

Once b_c and v are determined, the potential energy increase ΔP can be reduced to a simple expression in terms of the amplitude η and the load factor λ, (Refs.18, 19). In our case, where the bifurcation point is *symmetric* [1], this reduction yields:

$$\Delta P(t, \lambda; a) = (\lambda_c - \lambda)A'_2\eta^2 + A_4\eta^4 \qquad (5.6)$$

where the constants λ_c , A'_2, A_4 are defined by :

$$A'_2 = -\Delta P'_2(b_c) \; ; \; A_4 = \Delta P^0_4(b_c) - \{\Delta P^0_2(v) + \lambda_c \Delta P'_2(v)\} \qquad (5.7)$$

λ_c = value of the load parameter at buckling

The reduced form of the energy increase (5.6) represents an approximation that is accurate in some (small) neighborhood [2] of the bifurcation point, i.e., its accuracy increases when $|\eta| \rightarrow 0$; $|\lambda - \lambda_c| \rightarrow 0$. It is noted that the value of A'_2 is here defined in such a way that it is positive for the bifurcation point under consideration. (There are also bifurcation points for $\lambda < 0$ which means that for such points $A'_2 < 0$!)). The sign of A_4, which factor is determinate for the stability or instability of the buckling process, must also be positive in our case because we can still load the plate after the buckling point is reached.

The reduced form of the energy (5.6) is the simplest possible function that still represents the behavior of the structure in the neighborhood of the bifurcation point. From this function follows the basic bifurcation equation:

$$\frac{d}{d\eta}\{\Delta P(\eta; \lambda)\} = \frac{d}{d\eta}\{(\lambda_c - \lambda)A'_2\eta^2 + A_4\eta^4\} = 0 \qquad (5.7^a)$$

or

$$2(\lambda_c - \lambda)A'_2\eta + 4A_4\eta^3 = 0 \qquad (5.7^b)$$

It yields two solutions:

The pre-buckling state *I*: $\lambda \leq \lambda_c$; $\eta = 0$ $\qquad (5.8^a)$

---

[1] Symmetric means here that the branching diagram is symmetric around the state *I* : λD_0.

[2] The range of validity of expression (4.5) varies strongly with the problem at hand. For many plate problems it is relatively large, say in correspondence with: $|\lambda - \lambda_c|$ several times in excess of λ_c.

and

the postbuckling state *II*: $\lambda > \lambda_c$; $\eta^2 = -\frac{(\lambda_c - \lambda)A'_2}{2A_4}$ (5.8b)

The energy release rate was defined as:

$$G = -\{\frac{dP}{tda}\}_{\lambda = \text{constant}} = -\frac{\partial P}{t\partial a}$$

Along the state *I* this yields:

$$G = G_I(\lambda) = -\{\frac{\partial P}{t\partial a}\}_I = -\frac{\partial P[\lambda D_0]}{t\partial a} = \frac{K_I^2}{E} = (k_1)^2 \qquad (5.9)$$

where k_1 is a positive constant, i.e. $k_1 = K_I' = \frac{dK_I}{d\lambda}$.

Along the state *II* we get:

$$G = -\{\frac{\partial P}{t\partial a}\}_{II} = -\frac{\partial P[\lambda D_0]}{t\partial a} - \frac{\partial \Delta P[d;\lambda]}{t\partial a} \qquad (5.10)$$

Substitution of (5.5) gives:

$$G = \lambda(k_1)^2 - \frac{\partial}{t\partial a}\{(\lambda_c - \lambda)A'_2\eta^2 + A_4\eta^4\}$$

$$G = \lambda^2(k_1)^2 + \frac{\partial}{t\partial a}\{\frac{3}{4}(\lambda_c - \lambda)^2\frac{(A'_2)^2}{A_4}\} \qquad (5.11)$$

where use is made of the identity (5.8b). For simplicity we introduce:

$$\beta_1 = \frac{3}{2}\frac{(A'_2)^2}{A_4} \qquad (5.12)$$

which is a factor that contains the coefficients that govern the postbuckling solution (see (5.8b)). With this definition we get from (5.11):

$$G = \lambda^2(k_1)^2 + \beta_1\lambda_c^\circ(\lambda_c - \lambda) + \frac{1}{2}\beta_1^\circ(\lambda_c - \lambda)^2 \qquad (5.13)$$

where $()^\circ = \frac{\partial}{t\partial a}$, so that $\lambda_c^\circ = \frac{\partial}{t\partial a}\{\lambda_c\}$ and $\beta_1^\circ = \frac{\partial}{t\partial a}\{\beta_1\}$. Notice that the factor λ_c° that appears here can in principle be read from the graph in figure (7) and that it is clear that this factor must be negative.

From a computational point of view, expression (5.13) does not offer much prospective because it seems cumbersome to compute the derivatives λ_c° and β_1°. This is particular true for the factor β_1° which is built on the derivative b_c°. The significance of expression (5.13) rather lays somewhere else, i.e., in the general structure it reveals in terms of the dependency on the load factor λ. Notice that the relation in terms of λ agrees with the form of the computed solution in figure 11, i.e. it presents a quadratic function in terms of $\Delta\lambda = (\lambda - \lambda_c)$.

To obtain the rate of change of $G(\lambda)$ at the buckling point we determine the derivative of G with respect to λ (for 2a = constant):

$$\text{Along } \textit{I}: \quad \frac{\partial G}{\partial \lambda} = 2\lambda(k_1)^2$$

$$\text{Along } \textit{II}: \quad \frac{\partial G}{\partial \lambda} = 2\lambda(k_1)^2 - \lambda_c^\circ\beta_1 + \beta_1^\circ(\lambda - \lambda_c) \qquad (5.14)$$

Consequently at the buckling load λ_c, the slope to the $G(\lambda)$ curve undergoes a (finite) jump:

$$\left\{\frac{\partial G}{\partial \lambda}\right\}_{II} - \left\{\frac{\partial G}{\partial \lambda}\right\}_{I} = -\lambda_c^\circ\beta_1 > 0 \qquad (5.15)$$

which is a result that is completely confirmed by our calculations (figure 13).

5.2 The energy release rate in terms of the local crack tip solutions

In the foregoing we wrote the solution for the bifurcating branch as:

$$\mathbf{D}_{total} = \lambda\mathbf{D}_0 + \eta\mathbf{b}_c + \eta^2\mathbf{v} + O(\eta^3) \qquad (5.15)$$

It follows from our previous remarks that the components of this expansion can be written as:

$$\mathbf{D}_0 = \begin{pmatrix} b_x \\ b_y \\ 0 \end{pmatrix} \quad \mathbf{b}_c = \begin{pmatrix} 0 \\ 0 \\ b_{zc} \end{pmatrix} \quad \mathbf{v} = \begin{pmatrix} c_x \\ c_y \\ 0 \end{pmatrix} \qquad (5.16)$$

The subscript y and x refer here to the membrane or in plane displacements (u, v) while the subscript z refers to the out of plane displacements (w). We see that for our

problem, the buckling displacements $\mathbf{b}_c$, which are associated with the bending deformations, are exclusively in terms of (w), and that the two other vectors: $\mathbf{D}_0$ and the second order term v only contain components in terms of u and v. Consequently, in the initial stage of the buckling process the displacement field in a close region around the crack tip are expected to have the form:

$$\mathbf{u} = \mathbf{u}(x, y, z) = \lambda k_1 \begin{Bmatrix} \sqrt{r}\, Y(\theta) \\ \sqrt{r}\, \varsigma(\theta) \\ 0 \end{Bmatrix} + \eta k_{2b} \begin{Bmatrix} -z\sqrt{r}\, \omega_1(\theta) \\ -z\sqrt{r}\, \omega^*_1(\theta) \\ \frac{2}{3}\sqrt[3]{r}\, \omega_1(\theta) \end{Bmatrix} + \eta^2 k_2 \begin{Bmatrix} \sqrt{r}\, Y(\theta) \\ \sqrt{r}\, \varsigma(\theta) \\ 0 \end{Bmatrix} \tag{5.17}$$

where r, θ are the coordinates of a polar coordinate system at the crack tip, see figure 1. The precise specification of the functions Y, ς and so forth are immaterial at this stage of the discussion.

It is now noted that the energy release rate G can be expressed in terms of the integral (Irwin's representation) (Ref. 31):

$$G = \mathrm{Lim}_{\Delta a \to 0} \left\{ \int_0^{\Delta a} \int_{-\frac{t}{2}}^{\frac{t}{2}} \frac{1}{2} \sigma(x, z, a) u(\Delta a - x, z, a) dz\, dx \right\} \tag{5.18}$$

an expression in which only the local crack tip solution (5.17) plays a role. The specification of the functions that we need to evaluate under the integral sign are provided by the classical solutions for mode I stretch and mode I bending (see (Refs. 31, 32) and (Refs. 5, 38, 39) respectively). The components involved are given by:

$$\sigma_x(x, z, a) = \sigma_{xm}(x, a) + z\sigma_{xb}(x, a)$$

$$u(\xi, z, a) = u_{xm}(\xi, a) + z\kappa_{xb}(\xi, a) \tag{5.19a}$$

$$\xi = \Delta a - x$$

$$\sigma_{xm}(x, a) = \lambda k_1 \frac{1}{\sqrt{2\pi x}} + \eta^2 k_2 \frac{1}{\sqrt{2\pi x}} + (\text{irrelevant terms})$$

$$u_m(\xi, a) = \lambda k_1 \frac{1}{\sqrt{2\pi}} \sqrt{\xi} + \eta^2 k_2 \frac{1}{\sqrt{2\pi}} \sqrt{\xi} + (\text{irrelevant terms}) \tag{5.19b}$$

$$\sigma_{xb}(x,\ a) = \eta\ k_{2b}\frac{1}{\sqrt{2\pi x}} + \text{(irrelevant terms)}$$

$$\kappa_{xb}(\xi,\ a) = \eta\ k_{2b}\frac{1}{\sqrt{2\pi}}\sqrt{\xi}\ \frac{2z}{t} + \text{(irrelevant terms)} \qquad (5.19^c)$$

Carrying out the integration and taking the limit leads to the following result:

$$G = G_m + G_b$$

$$G = [\frac{1}{E}(\lambda k_1 + \Delta\lambda k_2)^2] + [\frac{2}{3}\frac{1}{E}\Delta\lambda\,(k_{2b})^2] \qquad (5.20)$$

where we note that the factor $(\frac{2}{3})$ before the bending term is actually not important, because it could very well be incorporated in k_{2b} and only has the character of a scaling factor.

The significance of this result, (5.20), and that given by (5.13) is the possibility to identify, i.e. to relate the membrane stress intensity factor $K_{Im}(\lambda)$ and the bending stress factor $K_{Ib}(\lambda)$, which are *local* parameters, to the corresponding *global* contributions in the energy release rate $G = G_m + G_b$. It follows by comparison of (5.13) and (5.20) that:

$$k_2 = k_1\{\sqrt{1 + \frac{E\beta^\circ_1}{(k_1)^2}} - 1\}$$

$$k_{2b} = \sqrt{\frac{3}{2}\{(-\lambda'_c)\beta_1 E - 2\lambda_c k_1 k_2\}} \qquad (5.21)$$

where it is understood that k_1 is given, i.e. by $k_1 = \frac{1}{\lambda_c}(K_{Ic})_I$ in accord with definition (5.9). Notice, that the expression for k_2 in (5.21) indicates that β_1 must be an increasing function of the crack length 2a.

These results obtained at (5.20 & 5.21) show how the intensity factors $K_{Im}(\lambda)$ and $K_{Ib}(\lambda)$ can be determined (in principle) from the global buckling analysis of section 5.2. But notice, that equation (5.20) also shows some light on the approximation that we introduced for the K_{Im} factor at (4.3). We can write (5.20) in the form:

$$G = [\frac{1}{E}(\lambda k_1 + \Delta\lambda k_2)^2]\left\{1 + \frac{\frac{2}{3}\frac{1}{E}\Delta\lambda(k_{2b})^2}{\frac{1}{E}(\lambda k_1 + \Delta\lambda k_2)^2}\right\} \qquad (5.22^a)$$

so that $\sqrt{G}$ becomes:

$$[K^*_{Im}]_{II} = \frac{1}{E}(\lambda k_1 + \Delta\lambda k_2)\left\{1 + \frac{\frac{2}{3}\Delta\lambda(k_{2b})^2}{(\lambda k_1 + \Delta\lambda k_2)^2}\right\}^{1/2} \qquad (5.22^b)$$

The "exact" expression for K_{Im} is:

$$[K_{Im}]_{II} = \frac{1}{E}(\lambda k_1 + \Delta\lambda k_2) \qquad (5.23)$$

It turns out that the results of our numerical calculations (figure 12) show very little deviation from this linear relation. This seems to indicate that the factor k_{2b}/k_1 is very small for the cases that we analyzed here. In other words, the bending part G_b of the energy release rate G is a negligeable factor in the postbuckling solution of the cracked plate and the approximate formula for the mode I intensity factor given by (4.3) must thus be fairly accurate.

5.3 Conclusions

It must be clear that the methods for nonlinear analysis that we described in this paper are very useful for the analysis of crack problems in thin walled plate and shell structures.

As far as the analysis of the centrally cracked plate is concerned, a number of interesting and we believe new facts were revealed regarding the physics of this problem. We can summarize these facts as follows:

-i- When the plate is loaded into the postbuckling state, the energy release rate, c.q. the stress intensity factor as a function of the load will bifurcate (with finite slope) from the relation that belongs to the (linear) prebuckling state.

-ii- The crack tip stress intensity along the post buckling path is always larger than it is along the pre-buckling path at the same value of the load. This effect increases with the crack length 2a.

-iii- The mechanical cause of this phenomenon must be sought in the redistribution of the membrane stress field during buckling process. This modification represents a more severe in-plane loading of the crack.

-iv- The relation between the membrane stress intensity factor K_{Im} and the intensity of the loading, which is a linear relation in the pre-buckling state, is again linear after buckling has taken place, at least, for values of the load not far in excess of the buckling load.

-v- The bending part of the energy release rate does not seem to play a noticeable role (as compared to the membrane part) in the cases considered here.

ACKNOWLEDGEMENT

REFERENCES

1. Riks E., den Reijer P.J., "A Finite Element Analysis of Cracks in a Thin Walled Cylinder under Internal Pressure", NLR TR 87021 U, National Aerospace Lab. NLR, the Netherlands, Jan. 1987.

2. Riks E., "Bulging Cracks in Pressurized Fuselages: A Numerical Study", NLR MP 87058 U, National Aerospace Lab. NLR, The Netherlands, Sept. 1987.

3. Riks E., Brogan F.A., & Rankin C.C., "Bulging Cracks in Pressurized Fuselages: A Procedure for Computation", December Meeting ASME, San Francisco, 1989. In: Analytical and Computational Models of Shells, Proceedings Winter Annual Meeting ASME (A.K. Noor, T. Belytschko, J.C. Simo eds.), C.E.D. Volume 3, The American Society of Mechanical Engineers, 1989.

4. Ansell, H., "Bulging of Cracked Pressurized Aircraft Structure," Ph.D. Thesis, Linkoping Institute of Technology, Sweden, April 1988.

5. Dong, Chen., " Bulging Fatigue Cracks in a Pressurized Aircraft Fuselage", PhD. Thesis, Delft University, Dept. of Aeronautics & Astronautics, Delft, The Netherlands, January, 1991.

6. Petyt M., "The Vibration Characteristics of a Tensioned Plate Containing a Crack", J. Sound Vib. 8, 377 (1968).

7. Dixon R. and Strannigan J. S.,. "Stress distribution and Buckling in Thin Sheets with Central Slits", Proc. 2nd. Int. Conf. on Fract., Brighton, 105 (1969).

8. Dyshel M. S., "Stability under Tension of Thin Plates with Cracks", Soviet Appl. Mech. **14**, 1169 - 1173 (1978)

9. Dyshel M. S., "Stability of Thin Plates with Cracks under Bi-axial Tension", Soviet Appl. Mech. **18**, 924 - 928 (1982)

10. Guz A. N., Kuliev G. G. and Tsurpal I.A.,"On Fracture of Brittle Materials from Loss of Stability near a Crack", Engng Fract. Mechanics, 10, 401 (1978).

11. Dal, Y. M., " Local Bending of a Stretched Rectangular Plate with a Crack", Soviet Appl. Mech. **17**, 120- 125 (1978)

12. Markström K., Storåkers B.,"Buckling of Cracked Members under Tension", Int. J. Solids Structures, Vol. 16, pp 217 - 229, 1980.

13. Rossmanith H. P., Troger H., Tschegg E., " Beulen und Reissen von Gezogenen Dünnen Blechen mit Innenrissen", Z. Flugwiss. Weltraumforsch. 5, (1981), Heft 1.

14. Fujimoto T. and Sumi S., "Local Buckling of Thin Tensioned Plate Containing a Crack", The Memoirs of the faculty of Engineering, Kyushu University, Vol. 12, pp. 355-370 (1982)

15. Fujimoto T. and Sumi S., "Elastic buckling of Center Cracked Plates under Tension", J. J. S. M. E. 52, 1582-1586 (1985)

16. Sih G. C. and Lee Y. D., " Tensile and Compressive Buckling of Plates Weakened by Cracks", Theor. Appl. Fracture Mech. 6, 129-138 (1986)

17. Shaw D., Huang Y. H. "Buckling Behavior of a Central Cracked Thin Plate under Tension" Engrg. Fracture Mechanics, Vol. 35. no 6. pp 1019 - 1027, 1990.

18. Budiansky B., " Theory of Buckling and Post-buckling Behaviour of Elastic Structures," in: "Advances in Applied Mechanics 14", edited by C.S. Yih, Academic Press, New York, 1974, 1-65.

19. Thompson J.M.T., Hunt G.W., " A General Theory of Elastic Stability," John Wiley & Sons, Ltd., (1973).

20. Almroth B.O., Brogan F.A., Stanley G.M.,"Structural Analysis General Shells", Vol.2 Users Instructions for STAGSC-1, LMSC D633873.

21. Rankin C. C. and Brogan F. A., "An Element Independent Corotational Procedure for the Treatment of Large Rotations," J. Pressure Vessel Techn., 108,pp. 165 - 174, (1986).

22. Rankin C. C. and Nour-Omid B., "The Use of Projectors to Improve Finite Element Performance," Computers & Structures, Vol. 30, No. 1/2, November, 1988, pp. 257-267.

23. Koiter W. T., " On The Nonlinear Theory of Thin Elastic Shells", Proc.Kon. Ned. Ak. v. Wetenschappen, 1- 54 (1966).

24. Koiter W.T., "General Equations of Elastic Stability for Thin Shells, Proc. Symp. on the Theory of Shells in honour of Loyd Hamilton Donnell, University of Houston, (1967).

25. Riks E., " The Application of Newtons Method to the Problem of Elastic Stability", J. Appl. Mech.,Vol. 39, pp. 1060-1066, Dec. 1972.

26. Rheinboldt W. C. and Riks E., "A Survey of Solution Methods for Finite Element Equations," In: State of the Art Surveys on Finite Element Technology, A.K. Noor, W.D. Pilkey eds., The American Society of Mechanical Engineers, 1983.

27. Riks E., "Some Computational Aspects of The Stability Analysis of Nonlinear Structures", Comp. Meth. in Appl. Mech. and Engng. 47. 219-259, 1984.

28. Riks E., "Progress in Collapse Analysis", Journal of Pressure Vessel Technology, Vol. 109/27 - 41,. Febr.1987.

29.Thurston G. A., Brogan F.A., Stehlin P., " Postbuckling Analysis Using a General Purpose Code", AIAA paper No. 85-079-CP. Presented at the AIAA/ASME/AHS 26th Structures, Structural Dynamics and Materials Conference, Orlando,Florida, April 15- 17, (1985).

30. Rankin C. C., Stehlin P. and Brogan F. A., "Enhancements to the STAGS Computer Code", NASA CR-4000, 1986.

31. Broek D., " Elementary Engineering Fracture Mechanics" Sijthof & Noordhoff, Alphen a/d Rijn - The Netherlands. (1987).

32 Owen D.R.J., Fawkes A.J., "Engineering Fracture Mechanics: Numerical Methods and Applications", Pineridge Press Ltd., Swansea, UK. (1983).

33. Parks D.M., "A Stiffness Derivative Finite Element Technique for Determination of Elastic Crack Tip Stress Intensity Factors", Int. J. Fracture 10, No. 4, 487-502, December (1974).

34. Hellen T.K., "On the Method of Virtual Crack Extensions", Int. J. Num. Meth. Engng. 9, No.1, 187-207 (1975).

35. LeFort P., deLorenzi H.G., Kumar V., German M.D., "Virtual Crack Extension Method for Energy Release Rate Calculations in Flawed Thin Shell Structures", Journal of Pressure Vessel Technology, Vol. 109/101-107, February 1987.

36. deLorenzi H.G., " Energy Release Rate Calculations by the Finite Element Method", Engineering Fracture Mechanics, Vol. 21, No. 1, 1985, pp. 129.

37. Hellen T. K., Blackburn W. S., "Non-linear Fracture Mechanics and Finite Elements", Eng. Comp., Vol. 4, pp. 2 - 14, March (1987).

38. Knowles, J. K. and Wang N.M.,"On the Bending of an Elastic Plate containing a Crack", Journal of Mathematics and Physics, Dec. 1961, pp. 223 - 236.

39. Sih G.C., Paris P., and Erdogan, F., "Crack Tip Stress Intensity Factors for plane Extension and Plate Bending problems", Journal of Applied Mechanics, Vol. 29, Trans. ASME, Vol. 84, series E, June 1962, pp. 306 - 312.